Eng Int Syst (2022) 3: 217–226


**Engineering**
***Intelligent Systems***

# Edge Recognition of Color Image Based on Super-Resolution Imaging Technology

**Shuai Ren*** **and Yu Zhang**

*College of Software Technology, Henan Finance University, Zhengzhou 450046, China*

The traditional edge recognition technology for color images is limited by the resolution constraints, resulting in blurred edges, and broken and uneven lines. Therefore, in this paper, a super-resolution imaging technology is used to overcome the resolution of traditional methods, and obtain sharper edges in color images. In order to better define the distinct colors in an image, edge recognition technology uses the double histogram color image for equalization processing. According to the changes in gray value, the corner feature of the image is extracted, and the edge model is constructed by a double interpolation algorithm to obtain the basic contour of the image. Finally, the contour features of the color image are identified by super-resolution imaging technology, and the edge recognition process is completed. The experiment is divided into two stages, and the selected test objects differ in terms of color, structure and content. After two rounds of testing, we can see that by applying the edge recognition technology proposed in this study, the edge of the color image is continuous and smooth; while the image edge obtained by three traditional technologies are not smooth; rather, it contains a large number of broken lines. The entropy of image information was used to evaluate the processed image, and it was found that the edge recognition technology applied in this study is capable of better edge detection.

Keywords: Super-resolution Imaging Technology, Color Image, Edge Recognition

## 1. INTRODUCTION

The vivid colors of an image can produce a visual impact, and can convey more information than a gray image. The eyes obtain a lot of visual information from an image, which can be processed quickly by the human brain, and in turn enables the human to make a judgment or draw a conclusion. When collecting visual information, in addition to paying attention to color, the most important thing is to judge the shape, size and position of the target in the image. The edge is the boundary between the target and the background, and it can also mark the overlapping boundary between the target and other items in the image, so it can describe the geometric properties of the target such as its contour, area, perimeter and spatial position in relation to other targets in the image (Krinidis et al., 2013). Therefore, the edge recognition technology applied to images is one of the most commonly-used operations in image segmentation and type recognition. By identifying the edges of separate items in the color image, image segmentation and type recognition can be achieved more accurately (Enshasy et al., 2019; Suryanarayana et al., 2019).

Super-resolution imaging technology generally refers to a type of image processing algorithm. With this technology, a particular algorithm is used to fuse multiple images containing similar, therefore redundant, information according to the single or multiple low-quality and low-resolution images obtained from the scene, but to a certain extent, there are different details to generate high-quality and high-resolution images. The key problem of reconstruction is to recover as much high-frequency information from the image as possible, because the high-frequency information yields some of the details, and only a large number of details can ensure the integrity of the information captured in the image

*Corresponding Author Email: rjxyrs@163.com

(Sidike et al., 2017). Super-resolution imaging technology can effectively suppress the random noise and blurring phenomenon in the process of image processing without increasing the cost incurred by the processing system. As a kind of far-field super-resolution imaging technology, super-resolution imaging technology is used mainly to detect details in microscopy, observation and imaging (Pandey and Ghanekar, 2019). Super-resolution imaging technology involves the selection of nonlinear stimulated radiation of light molecules. The whole process consists of two steps: in the first step, the laser beam used for focusing can excite a specific beam and generate a difference curve at the junction area of the image edge area; in the second step, the image edge is defined according to the same type of light wave.

Edge detection in image processing is mainly for the realization of computer-automated understanding and recognition of images. Regardless of the purpose, the accuracy of edge detection is very important. At present, image edge detection technology is applied in various fields, and some mature algorithms in special fields are embedded in a single-chip microcomputer for commonly-used portable devices. However, these algorithms are more or less limited. Most of them are gradient operators for local calculation of image pixels, which are very sensitive to noise. The extracted edge is not a single pixel edge (Aymaz and Köse, 2019; Singh et al., 2018; Voynov et al., 2019; Wen et al., 2019). In addition, this method has a general problem in terms of the central pixel, as these operators cannot obtain the direction of the edge points. Therefore, in view of the current aforementioned problems, a color image edge recognition method based on super-resolution imaging technology is proposed and tested to determine its effectiveness as a means of image segmentation and type division.

## 2. ALGORITHM DEFINITION

In this study, the edge recognition technology for color images requires a hyperbolic interpolation algorithm. (Irfan et al., 2019; Ishtiaq et al., 2019). The interpolation equation is:

$$G(i+x, j+y) = (1-x)(1-y)G(i, j) + (1-x)\\ yG(i, j+1) + x(1-y)G(i+1, j) + xyG(i+1, j+1) \tag{1}$$

In Equation (1), $x$ and $y$ are floating-point numbers of [0,1) interval. Although bilinear interpolation can effectively overcome the mosaic phenomenon of nearest neighbor interpolation, the high-resolution image obtained is still fuzzy at the edges and other details are unclear. Hence, using the hyperbolic interpolation algorithm to build the edge detection model, the super-resolution imaging technology is applied to identify the contour edge.

## 3. EDGE RECOGNITION TECHNOLOGY OF COLOR IMAGE BASED ON SUPER-RESOLUTION IMAGING TECHNOLOGY

### 3.1 Image Color Equalization With Double Histogram

According to the RGB color space of a color image, the principle of double histogram equalization is applied to images with R, G and B components, and then traditional histogram equalization processing is carried out to adjust the brightness range of score quantum image, and then the gray level of balanced image is evenly distributed to realize the second gray level mapping; finally, the processed components are fused with other components after filtering. The color restoration factor is introduced to merge the sub-image components in order to obtain the enhanced color image (Shubham and Bhandari, 2019). For a color image to be enhanced, $I$ is recorded as $g$. The color components of structural element CC are R, G and B respectively. According to the principle of image flexible morphology, the equations of high cap filtering and low cap filtering are obtained as follows. The color components of structural elements are R, G and B respectively. According to the principle of image flexible morphology, the equations for obtaining high cap filtering and low cap filtering are:

$$\begin{cases} \widehat{L} = g - (g \circ [B, A, s]) \\ \breve{L} = g - (g \bullet [B, A, s]) \\ L = g + \widehat{L} - \breve{L} \end{cases} \tag{2}$$

In Equation (2), $L$ is the enhanced color image. In other words, each component image of $I$ is enhanced by the third equation in the above equations, and the color image $F$ is obtained after fusion. For $F$, the gray images of color components R, G and B are $R_r$, $G_g$ and $B_b$ respectively. For each gray image, the gray level is $J_i = (i = r, g, b)$. If $m_s$ is the number of pixels with gray level of $r_s$, the equation for the calculation of probability density function is:

$$P_s(r_s) = \frac{m_s}{m} \tag{3}$$

In Equation (3), $0 \le r_s \le 1$, $s = 0, 1, \ldots, J_i - 1$. The discrete form of the known transformation function is:

$$f_s = T(r_s) = \sum_{i=0}^{s} p_x(r_i) = \sum_{i=0}^{s} P_s(r_s) \tag{4}$$

In Equation (4), $0 \le r_s \le 1$, $s = 0, 1, \ldots, J - 1$. Combined with the above equation, the calculation expression of probability density function after equalization is obtained with:

$$p_x(f) = \left[ p_x(r) \frac{dr}{df} \right]_{r=T^{-1}} \tag{5}$$

It is known that the transformation function is $F = T(r) = \int_0^x p_x(r)\,dr$. According to the above equation and Leibniz criterion (Jaiswal et al., 2019), the derivation of the above equation is obtained:

$$\frac{df}{dr} = \frac{dT(r)}{dr} = \frac{d}{dr}\left[\int_0^x p_x(r)dr\right] = p_x(r) \tag{6}$$

By substituting Equation (6) into Equation (5), we can get:

$$p_x(r) = \left[\frac{df}{dr} \times \frac{dr}{df}\right]_{r=T^{-1}(s)} = 1 \tag{7}$$

This shows that the transformed $f$ has a uniform density in the definition domain $p_x(r)$, and its significance to image enhancement is that the dynamic range of image pixels is increased, and the overall visual effect of the image is improved. After the transformation process, the first gray-scale mapping is realized, and the image after equalization is $S$. At this time, the actual gray-scale of the image is recorded as $\tilde{J}$. Also, the gray-scale and probability density of the image $\tilde{J}$ are evenly distributed, which is evident in the enhanced image where the dynamic range of each pixel is increased, and the brightness and visual effect are improved. However, in the actual image processing, because some gray levels have no pixel distribution and other gray levels have concentrated pixel distribution, this causes the decreased gray level to appear as a gray level fault phenomenon, and the combination of adjacent gray levels also makes the image appear to lack details. In order to solve this problem, the actual gray level $\tilde{J}$ after equalization is uniformly distributed. The actual gray level is:

$$\tilde{J} = \begin{cases} \sum_{i=0}^{255} J_i + 1 & m_i \neq 0 \\ \sum_{i=0}^{255} J_i + 1 & m_i = 0 \end{cases} \tag{8}$$

The following transform function is used to distribute the actual gray level uniformly, and perform the second gray level mapping:

$$\tilde{f}_s = \tilde{T}_s = j \cdot \frac{255}{\tilde{J}_i} \tag{9}$$

In Equation (9), $j = 0, 1, \ldots, s$; $i = r, g, b$. The double equalization component image $D_i$ can be obtained by Equation (9). By calculating the proportion of the total gray levels of R, G and B sub quantum images of the original image to the total gray levels of the original color, the processed $D_r$, $D_g$ and $D_b$ are combined. Set $R(i, j)$, $G(i, j)$ and $B(i, j)$ to represent the gray level of the R, G and B component image of the input image respectively. For each pixel in the original image, there is a certain proportional relationship with the gray level of the corresponding R, G and B quantum image. Set $\tilde{R}(i, j)$, $\tilde{G}(i, j)$ and $\tilde{B}(i, j)$ to represent the gray level of the component sub-image processed by the double histogram equalization respectively. The proportion of the gray level of the R, G and B component after the enhancement remains unchanged, then:

$$R(i, j)\colon G(i, j)\colon B(i, j) = \tilde{R}(i, j)\colon \tilde{G}(i, j)\colon \tilde{B}(i, j) \tag{10}$$

In the actual enhancement process, because Equation (10) does not necessarily hold, the color of the processed image is distorted. Hence, the color restoration factor is introduced to enhance the color image at night, namely:

$$\begin{cases} \mu_k(i, j) = h\left[\partial \tilde{I}_s(i, j)\right] \\ \tilde{I}_s(i, j) = \frac{I_s(i,j)}{\sum_{m=1}^{N} I_s(i,j)} \end{cases} \tag{11}$$

In Equation (11), $s = r, g, b$, $N = 3$; $\mu_k$ is the color recovery coefficient of a channel in $(r, g, b)$; $I_s(i, j)$ is the total gray level of $s$ sub image; $N$ is the number of R, G and B components; $I_s(i, j)$ is the gray level of the original image; $h$ is the mapping function of color space. Through the above calculation process, the double histogram equalization of the color image is realized.

## 3.2 Corner Feature Extraction

The corner features are extracted from the enhanced color image (Nodari, et al. 2012). The known corner point is the local maximum point whose curvature exceeds a certain threshold value on the contour line of the target. If a small offset of a point in any direction causes a great change in the gray scale, then that the point is a corner (Wen et al., 2020; Li and Gao, 2019). The following equation determines the change of gray value:

$$H(a, b) = \sum_{x,y} c(x, y)[\tilde{I}(x + a, y + b) - \tilde{I}(x, y)]^2 \tag{12}$$

In Equation (12), $c(x, y)$ is the window function; $\tilde{I}(x, y)$ is the gray level of the original position of the enhanced image; $\tilde{I}(x+a, y+b)$ is the gray level of the moved image. According to the expansion of Taylor series (Borjigin and Sahoo, 2019), the Equation (12) can be approximately expressed as:

$$H(a, b) \cong [a, b]M \begin{bmatrix} a \\ b \end{bmatrix} \tag{13}$$

$$N = \sum_{x,y} c(x, y) \begin{bmatrix} \tilde{I}_x^2 & \tilde{I}_x\tilde{I}_y \\ \tilde{I}_x\tilde{I}_y & \tilde{I}_y^2 \end{bmatrix} = \begin{bmatrix} N_{11} & N_{12} \\ N_{12} & N_{22} \end{bmatrix} \tag{14}$$

In Equation (14), $\tilde{I}_x$ and $\tilde{I}_y$ are the gray level of the point and the partial derivatives in the direction of $x$ and $y$, respectively. A corner can be detected using this equation:

$$\varphi(x, y) = \frac{N_{11} \cdot N_{22} - N_{12}^2}{N_{11} + N_{22}} \tag{15}$$

$\varphi(x, y)$ will be regarded as the corner if it is greater than a certain threshold value, and if it is the local maximum value within a certain window width. Figure 1 depicts the extraction of a corner.

As shown in Figure 1, corner features are extracted according to the contour of the color image. The image is divided into different regions according to its position or structure, and then the basic contour of the image is obtained according to the region.

## 3.3 Double Interpolation Algorithm to Build Edge Model to Obtain Image Basic contour

Edges contain rich information, and therefore are an important component of images. An edge has several specific structural properties: the image gradient is very different in the parallel and vertical directions of the edge, that is, anisotropy; an edge has continuity, that is, there must be other edge points around one edge point; an edge can be indicated by many short lines, etc. By means of the proposed double interpolation algorithm, the edge model is established to obtain the basic contour of the image.

There is no very strict definition of color image edge. Broadly speaking, the point with a sudden change in brightness, the point with a sudden change in color saturation and the point with a local maximum gradient in each channel of color image can be considered as an edge point in a color image (Gedkhaw et al., 2019). According to the known edge detection algorithm, the edge of a color image is divided into five categories: object edge, which generally appears at the discontinuity of continuous surface; specular edge, which appears at the special angle of light source due to the material characteristics; reflective edge, which generally occurs due to the change of surface material in the image; shadow edge, which occurs due to the discontinuity of incident light intensity; and the occluded edge which is the boundary between the object and the background from the perspective view. The occluded edge appears only in a certain perspective, and it is not an edge as such. Figure 2 shows the edge schematic of a color image.

When processing digital images in different application scenarios, different edge types may need to be considered. For example, in target recognition, we need an object edge and an occluded edge. In stereo vision, we need to pay attention to the edge of the object, reflection edge and shadow edge; the back highlight edge and occluded edge appear only under specific circumstances. It is known that color images are based on RGB color space. In a color image, if the value of each optical channel is regarded as a separate image, it can be compared to a gray image (Tuna et al., 2018). The value of each pixel in the gray image indicates the different intensity of the gray scale. The ideal edge is the place where the gray scale value jumps. However, in practice, the edge often becomes fuzzy. The gray scale change is not a step shape, but a slope shape. There is a transition region with a certain width, which leads to the deviation of edge point positioning. Therefore, as indicated in the last two sections, the deviation is minimized. The equation used to calculate the edge model established by the double interpolation algorithm is:

$$G(x) = \begin{cases} \exp\left[-\frac{(x-l_0)^2}{2\lambda^2}\right] & x > l_0 \\ 1 \quad |x| \le l_0 \\ \exp\left[-\frac{(x+l_0)^2}{2\lambda^2}\right] & x < -l_0 \end{cases} \tag{16}$$

In Equation (16), $G(x)$ is the edge contour parameter; $x$ is the corner coordinate of the extracted image; $l_0$ is the total length of the contour; $\lambda$ is the contour scale of the parallel direction and the vertical direction. The basic contour of the image is obtained by using the upper edge model.

## 3.4 Edge Recognition Based on Super-Resolution Imaging Technology

From the obtained image contour, the edge of the color image is identified by means of super-resolution imaging technology. Based on the basic principle of geometric optics in super-resolution imaging technology, the focusing characteristics of microspheres in image edge recognition are analyzed through ray tracing. As shown in Figure 3, a ray parallel to the optical axis incident on the microsphere at a height of $h$ and refracted, and then intersected with the microsphere and the optical axis at points A, B and C in turn. $z$ is the radius of the microsphere, $z_1$ is the refractive index of the microsphere and $r$ is the refractive index of the external medium. Focal length $q$ is defined as the distance from the center of the sphere to point C (Shivagunde and BIswas, 2019).

According to the refraction law and geometric relationship, the focal length of the microsphere can be obtained by simply pushing it down. The angle is obtained with:

$$\alpha = 2\left(\sin^{-1}\cdot\frac{h}{r} - \sin^{-1}\cdot\frac{z_1\cdot h}{zr}\right) \tag{17}$$

According to Equation (16) and Equation (17), the focal length of the microsphere in the identification of contour edge by super-resolution imaging technology is obtained with:

$$q = \frac{h}{\sin\alpha}\cdot G(x)^{-1} \tag{18}$$

It can be seen from Equation (18) that the light with different height $h$ will focus on different positions on the optical axis; that is, there is spherical aberration in the microsphere itself. The focal length is usually the focal point of paraxial light passing through the microsphere. By paraxial approximation of Equation (17), the expression of focal length is obtained with:

$$q = \frac{zr}{2(z - z_1)}\cdot G(x)^{-1} \tag{19}$$

In Equation (19), the focal length of the microsphere is directly proportional to the radius, and decreases with the increase of the refractive index difference $z/z_1$ between the microsphere and the external medium. When $z/z_1$ is greater than 2, the focal length is less than $r$, and the focal point is in the ball. When the refractive index of the microsphere and the external medium is changed at the same time and the value of

**Figure 1** Corner extraction effect.

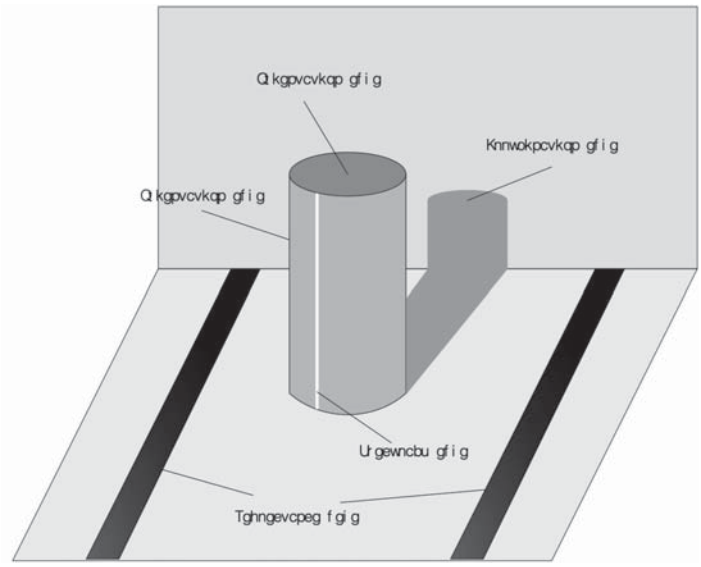


**Figure 2** Diagram of edges in a color image.

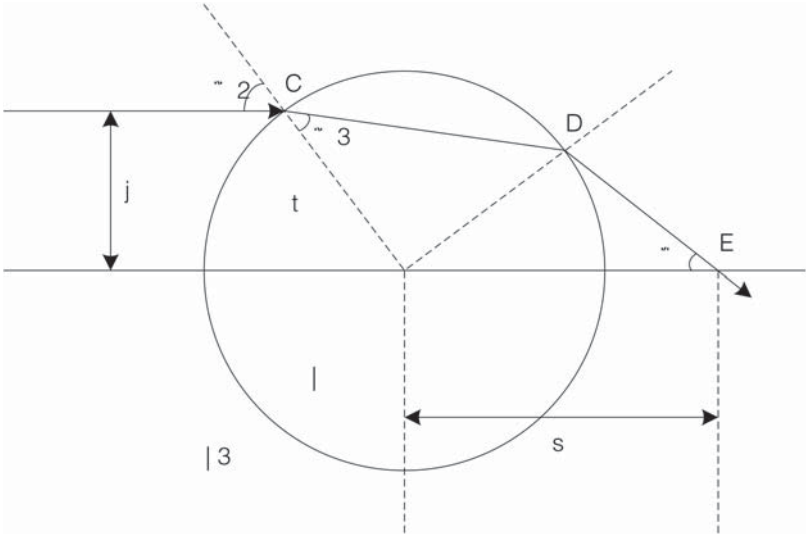


**Figure 3** Microsphere focusing diagram.

**Table 1** Criteria for selection of experimental test objects.

| Number | Selection requirements | Stage one | The second stage |
|---|---|---|---|
| 1 | Color difference | Less | Too large |
| 2 | Image structure | Single | Complex |
| 3 | Composition information | Less | Excessive |

**Figure 4** Test object for the first-stage experiment.

$z/z_1$ remains constant, the focal length will not be changed. This demonstrates that super-resolution imaging technology can achieve edge recognition in color images.

## 4. EXPERIMENTAL DETECTION

In order to verify the accuracy of the color image edge recognition method based on super-resolution imaging proposed in this paper, an experiment is conducted for the purpose of comparison. The color image edge recognition technology proposed in this paper is compared with three traditional edge recognition technologies (Gedkhaw et al., 2019, Irfan et al., 2019; Ishtiaq et al., 2019). According to the smoothness of the image edge contour connection, four kinds of recognition are used to determine the reliability of other technologies. In the experiment, the recognition technology proposed in this study is used as group A, and three traditional technologies are used as group B (Gedkhaw et al., 2019), group C (Irfan et al., 2019) and group D (Ishtiaq et al., 2019). First, the experimental test environment is set up, then the experimental test object is selected. The criteria for the selection of test objects are shown in Table 1.

### 4.1 Phase I Test

As the test object, the chosen color image has a simple structure, small color difference and less content information, as shown in Figure 4.

Four kinds of color image edge recognition technologies are applied to identify the edge of the test object shown in Figure 4. Figure 5 shows the results of the second-stage test comparison.

The test results for the four groups of experiments show that the image edge recognition technology proposed in this study extracts the corner features of the enhanced image, and uses super-resolution imaging technology to obtain more detailed image edges from the image contour, ensuring that all curves are continuous and uninterrupted. However, the three traditional techniques have poor resolution, the edge of the color image is blurred, and the curve is broken or lost. As evident, the image edge recognition technology proposed in this paper produces a smoother image.

### 4.2 Second Stage Test

After the first phase of the relatively easy experimental test, as the experimental test object, a color image is selected that has a complex structure, more color contrast and rich content, as shown in Figure 6.

Four kinds of color image edge recognition technologies are used to identify the edge of the test object shown in Figure 6. Figure 7 shows for comparison the results of the second-stage test.

From the observation of the recognition curve, we can see that for group A, super-resolution imaging is carried out according to the corner features extracted after image enhancement, so that the recognition curve is continuous and uninterrupted. But the traditional technology is limited by the resolution, the edge curve of the recognition image is completely broken, and lost, and cannot convey the content of the original image.

(a) Test results obtained by group A

(b) Test results obtained by group B

(c) Test results obtained by group C

(d) Test results obtained by group D

**Figure 5** Comparison results of the first-stage experiment.

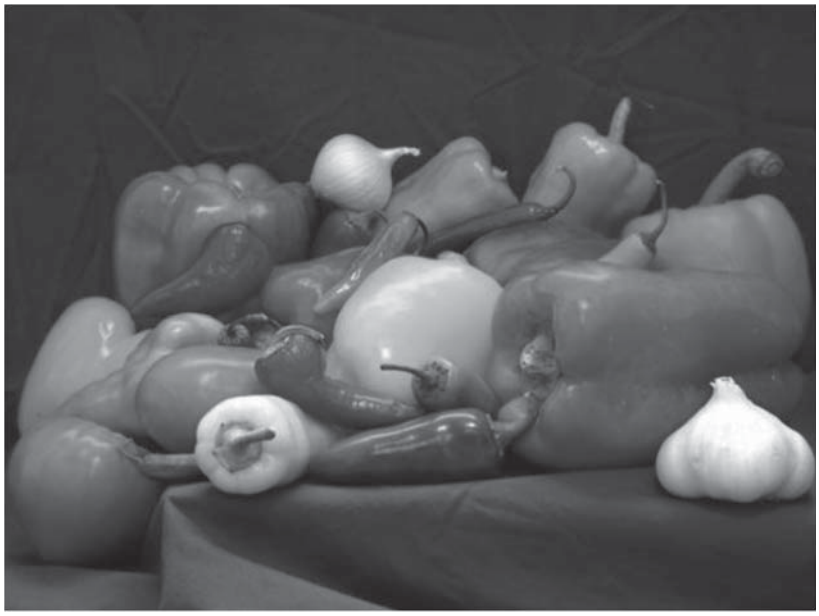

**Figure 6** Test object for the second-stage experiment.

### 4.3 Image Evaluation

Shannon, the father of information theory, proposed information entropy in 1984. When the information entropy equation is applied to image processing, it describes the average information provided by an image. Hence, image entropy can only represent the aggregated features of gray distribution in an image, but not the spatial features of gray distribution. The two-dimensional entropy of an image can be formed by adding a feature to the one-dimensional entropy, but the feature must be able to represent the spatial characteristics of the image distribution to a certain extent. The information entropy of an image consists of the average number of bits of an image at a certain gray level. The unit of image entropy is bit / pixel, which is the average information conveyed by an image. For the discrete two-dimensional image, the mathematical expression is:

$$H(p) = -\sum_{i,j} p(i, j) \ln p(i, j) \tag{20}$$

In Equation (20), $p(i, j) = x(i, j) \sum_{i,j} x(i, j),\ x(i, j)$ is the pixel value of image center point (i, j) and $H(p)$ is the entropy value of the image.

Then the image entropy calculation method above is used to calculate the entropy value of each algorithm in the pepper image to obtain the edge image; this is combined with the entropy value of the edge image previously detected in the mushroom image to obtain the values listed in Table 2, so as to determine the effectiveness of the detection.

From the data in Table 2, it can be seen that the entropy value of image edges detected by the Group C algorithm is the lowest, the entropy value of edge image detected by the algorithm designed in this paper is the highest, and the entropy value of the Group B algorithm and the Group D algorithm are higher than that of the traditional Group C algorithm, indicating that the edge detection accuracy of the algorithm designed in this paper is good, yielding the same result as that obtained by subjective evaluation.

## 5. CONCLUSIONS

In this paper, a color image is taken as the main research object, and the edge detection and classification of a color image are analyzed and discussed. Subsequently, a color image edge recognition technology based on super-resolution imaging technology is proposed. The basic contour of an image is obtained by enhancing the color image and extracting corner points, and then the contour edge of original image is recognized by super-resolution imaging technology to enhance the image, enabling the continuity and fluency of the recognition curve to be obtained. Although some problems in the traditional methods have been resolved, there are still some areas for improvement. On the one hand, the proposed algorithm has certain limitations, and other technical assistance is needed to improve the detection of image edges. Hence, there is a need for more in-depth research and the design of a more general adaptive edge detection algorithm. At present, the research on the whole-vector method applied to color images still has shortcomings in terms of theory, and there is no practical and effective algorithm to solve the practical problems. In order to conduct research on the whole-vector approach to color images, we need to improve the theory and achieve real-color image processing.

## ACKNOWLEDGEMENT

The research is supported by: Henan Higher Education Teaching Reform Research and practice project: Research and practice of applied software talent training mode based on the integration of KSIC (knowledge, skills, innovation and characteristics) (No. 2019SJGLX161).

(a) Test results obtained by group A

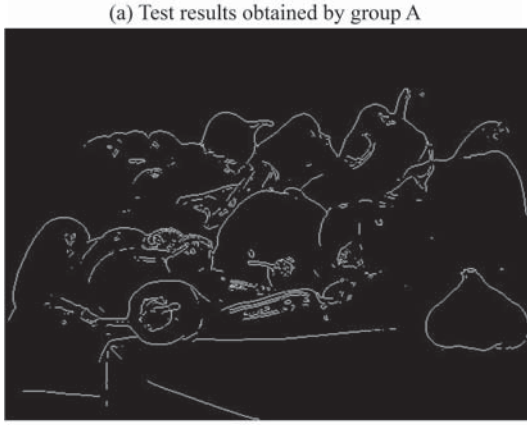

(b) Test results obtained by group B

(c) Test results obtained by group C

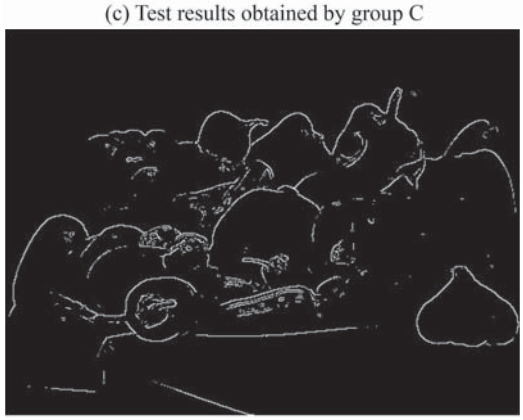

(d) Test results obtained by group D

**Figure 7** Comparison results of the second-stage experiment.

**Table 2** Entropy value of each detected edge.

| Experiment | Group A | Group B | Group C | Group D |
|---|---|---|---|---|
| The first stage | 0.5687 | 0.3669 | 0.2698 | 0.4512 |
| The second stage | 0.6704 | 0.5638 | 0.2358 | 0.4102 |

## REFERENCES


1. Aymaz, S.; Köse, C. 2019. A novel image decomposition-based hybrid technique with super-resolution method for multi-focus image fusion. *Information Fusion*, 45, 113–127.
2. Borjigin, S., Sahoo, P.K. 2019. Color image segmentation based on multi-level Tsallis–Havrda–Charvát entropy and 2D histogram using PSO algorithms. *Pattern Recognition*, 92, 107–118.
3. Enshasy H, Al-Haija Q.A., Al-Amri H., Al-Nashri M., Al-Muhaisen S. 2019. A Schematic Design of HHO Cell as Green Energy Storage. *Acta Electronica Malaysia, 3*(2), 09–15.
4. Gedkhaw, Ea., Ketcham, Ma. 2019. A super-resolution image reconstruction using triangulation interpolation in feature extraction for automatic sign language recognition. In: *2019 Research, Invention, and Innovation Congress* (RI2C). IEEE, 1–6.
5. Irfan, M.A., Khan, S., Arif, A., et al. 2019. Single image super resolution technique: An extension to true color images. *Symmetry, 11*(4), 464.
6. Ishtiaq S., Sajid A., Wagan R.A. 2019. RFID Technology Working it's Applications and Research Challenges. *Acta Informatica Malaysia, 3*(2), 05–06.
7. Jaiswal, V., Sharma, V., Varma, S. 2019. An implementation of novel genetic based clustering algorithm for color image segmentation. *Telkomnika, 17*(2), 1461–1467.
8. Krinidis, S., Krinidis, M., Chatzis, V. 2013. Fast and robust fuzzy active contours. *Engineering Intelligent Systems, 21* (2–3), 133–146.
9. Li F., Gao X. 2019. Optimal Methodologies. *Information Management and Computer Science*, *2*(1), 01–03.
10. Nodari, A., Gallo, I., Vanetti, M., et al. 2012. Color and texture indexing using an object segmentation approach. *Engineering Intelligent Systems, 20*(1–2), 47–57.
11. Pandey, G.; Ghanekar, U. 2019. Classification of priors and regularization techniques appurtenant to single image super-resolution. *The Visual Computer*, 1–14.
12. Shivagunde, S., BIswas, M. 2019. Saliency guided image super-resolution using PSO and MLP based interpolation in wavelet domain. In: *2019 International Conference on Communication and Electronics Systems* (ICCES). IEEE, 613–620.
13. Shubham, S., Bhandari, A.K. 2019. A generalized Masi entropy based efficient multilevel thresholding method for color image segmentation. *Multimedia Tools and Applications, 78*(12), 17197–17238.
14. Sidike, P., Krieger, E., Alom, M.Z., et al. 2017. A fast single-image super-resolution via directional edge-guided regularized extreme learning regression. *Signal, Image and Video Processing, 11*(5), 961–968.
15. Singh, K.K.; Bajpai, M.K.; Pandey, R.K. 2018. A novel approach for enhancement of geometric and contrast resolution properties of low contrast images. *IEEE/CAA Journal of Automatica Sinica, 5*(2), 628–638.
16. Suryanarayana, G.; Dhuli, R.; Yang, J. 2019. Single image super-resolution algorithm possessing edge and contrast preservation. *International Journal of Image and Graphics, 19*(4), 1950024.
17. Tuna, C., Unal, G., Sertel, E. 2018. Single-frame super resolution of remote-sensing images by convolutional neural networks. *International Journal of Remote Sensing, 39*(8), 2463–2479.
18. Voynov, O., Artemov, A., Egiazarian, V., et al. 2019. Perceptual deep depth super-resolution. In *Proceedings of the IEEE International Conference on Computer Vision,* 653–5663.
19. Wen, F., Min, F., Zhang, Y.J., et al. 2019. Crude oil price shocks, monetary policy, and China's economy. *International Journal of Finance & Economics, 24*(2), 812–827.
20. Wen, F., Wu, N., Gong, X. 2020. China's carbon emissions trading and stock returns. *Energy Economics*, 86, 104627.